Genetically engineered mesenchymal stromal cells producing IL-3 and TPO to further improve human scaffold-based xenograft models

M. Carretta[1#], B. de Boer[1#], J. Jaques[1], A. Antonelli[1], S.J. Horton[1,2], H. Yuan[3], J.D. de Bruijn[4], R.W.J. Groen[5], E. Vellenga[1], and J.J. Schuringa[1*]

[1]Department of Experimental Hematology, Cancer Research Centre Groningen (CRCG), University Medical Centre Groningen, University of Groningen, The Netherlands. [2]Current address: Department of Haematology, Cambridge Institute for Medical Research, University of Cambridge, Cambridge, UK. [3]Xpand Biotechnology BV, Bilthoven, The Netherlands. [4]Queen Mary University of London, School of Engineering and Materials Science (SEMS), Mile End Road, E1 4NS London, UK. [5]Dept of Hematology, VU University Medical Center, Amsterdam, The Netherlands. [#]Shared authors.

Short title: Genetically engineered MSCs in humanized xenografts

***Address correspondence to:** Prof. dr. Jan Jacob Schuringa (PhD), j.j.schuringa@umcg.nl

Department of Experimental Hematology, University Medical Centre Groningen (UMCG), Hanzeplein 1, DA13, 9700RB Groningen, The Netherlands

E-mail address: j.j.schuringa@umcg.nl; Phone: +31 50 3619391; Fax: +31 50 3614862

Category: Microenvironment and niche

Word count abstract: 249 words,

Word count text: 3505

Abstract

Recently, NOD-SCID IL2Rγ$^{-/-}$ (NSG) mice were implanted with human mesenchymal stromal cells (MSCs) in the presence of ceramic scaffolds or matrigel in order to mimic the human bone marrow (BM) microenvironment. This approach allowed the engraftment of leukemic samples that failed to engraft in NSG mice without humanized niches and resulted in a better preservation of leukemic stem cell self-renewal properties [1-3]. To further improve our humanized niche scaffold model, we genetically engineered human MSCs to secrete human IL-3 and TPO. *In vitro*, these IL-3 and TPO-producing MSCs were superior in expanding human cord blood (CB) CD34^{+} hematopoietic stem/progenitor cells. MLL-AF9-transduced CB CD34^{+} cells could efficiently be transformed along myeloid or lymphoid lineages on IL-3 and TPO-producing MSCs. *In vivo*, these genetically engineered MSCs maintained their ability to differentiate into bone, adipocytes and various other stromal components. Upon transplantation of MLL-AF9-transduced cord blood CD34^{+} cells both AML and ALL developed in engineered scaffolds, whereby a significantly higher percentage of myeloid clones was observed in the mouse compartments compared to previous models. Engraftment of primary AML, B-ALL and biphenotypic acute leukemia (BAL) patient samples was also evaluated and all patient samples could efficiently engraft, whereby the myeloid compartment of the BAL samples was better preserved in the human cytokine scaffold model. In conclusion, we show that we can genetically engineer the ectopic human BM microenvironment in our humanized scaffold xenograft model. This approach will be useful to functionally study the importance of niche factors for normal and malignant human hematopoiesis.

Highlights

- Human IL-3- and TPO-expressing MSCs support expansion of human $CD34^+$ cells.
- Genetically engineered MSCs are capable to form bone and stromal components *in vivo.*
- Humanized xenograft models producing IL3/TPO support growth of patient samples.

Introduction

Over the past decades, mouse xenograft models have significantly contributed to a better understanding of normal and malignant human hematopoiesis. The generation of immunodeficient mouse strains like the NOD-SCID IL2Rγ$^{-/-}$ (NSG) allowed researchers to functionally define human hematopoietic stem cells (HSCs) and their malignant counterpart [4-6]. These models also served as preclinical models for drug testing [7].

Even though different subtypes of primary human acute myeloid leukemia (AML) samples can expand in these models, major limitations still exist as well. For 30-40% of AML samples engraftment remains challenging, especially for the favorable and intermediate risk groups [8-10]. This might be explained by the influence of the murine microenvironment and the absence of species-specific human factors. NOD-SCID and NSG transgenic mice expressing human factors such stem cell factor (SCF), granulocyte-macrophage colony-stimulating factor (GM-CSF), Interleukin-3 (IL-3), and thrombopoietin (TPO) have been developed and allowed an increase in the engraftability rate of primary AML samples [11-14]. Furthermore, the expression of human SCF, GM-CSF and IL-3 allowed AML development upon transplantation of cord blood (CB) CD34^{+} cells expressing the MLL-AF9 oncogene [15]. More recently, a series of additional models have been developed [16-22]. For instance, MISTRG mice were developed whereby human macrophage colony-stimulating factor (M-CSF), IL-3, GM-CSF and TPO were knocked-in in their respective mouse loci, together with a BAC-transgene encoding for human SIRPα, supporting the development and function of innate immune cells *in vivo* [16].

Yet, in these human cytokine mice essential human niche-specific factors might still be lacking. Also, the interaction of hematopoietic cells with specific human niche components (such as adipocytes, osteoblast or endothelial cells) might be critically important to allow homing and long-term self-renewal of HSCs. In order to reconstruct a human bone marrow (BM) microenvironment in immunodeficient mice, we recently developed an approach whereby ceramic scaffolds coated with human mesenchymal stromal cells (MSCs) were implanted subcutaneously in NSG mice [1,3]. We observed that CB $CD34^+$ cells expressing BCR-ABL or MLL-AF9 could efficiently induce both AML and acute lymphoblastic leukemia (ALL) in these human BM scaffold-based xenografts (huBM-sc). Furthermore, a large cohort of patient samples covering all important genetic and risk subgroups successfully engrafted in this model, whereby stem cell self-renewal properties were better maintained as determined by serial transplantation assays and genome-wide transcriptome studies.

Although the presence of an ectopic human BM niche presents clear advantages compared to normal NSG mice, some key issues still remain. For example, there are a number of growth factors that are not produced by MSCs, including TPO and IL-3. Here, we investigated whether we could genetically engineer MSCs to produce such factors and evaluated these modified MSCs *in vitro* and *in vivo* in humanized scaffold xenograft models. We engineered MSCs to overexpress IL-3 and TPO (henceforth referred to as cyto-MSCs) that efficiently supported expansion of human $CD34^+$ stem/progenitor cells *in vitro*. Furthermore, these cyto-MSCs were functionally capable to form bone, adipocytes and various other stromal components *in vivo* and efficiently supported growth of AML, B-cell ALL (B-ALL) and biphenotypic patient samples (BAL). Lastly, we

found that the presence of IL-3 and TPO impacts on the lymphoid versus myeloid output in a CB MLL-AF9 *in vivo* model.

Material and Methods

Humanized scaffold niche xenograft model

The ectopic bone model was established as described previously [1,3,23]. Briefly, four hybrid scaffolds consisting of three 2–3 mm biphasic calcium phosphate particles loaded with human MSCs and/or IL-3- and/or TPO-expressing MSCs were implanted subcutaneously into 6 to 8 weeks old female NOD.Cγ-Prkdcscid Il2rγtm1Wjl/SzJ (NSG) mice. Six to eight weeks after scaffold implantation, different cell doses (patient samples or CB models) ranging from 0.9×10^5 to 4×10^6 were directly injected into the scaffolds during primary and secondary transplantations as indicated in the text. Human CD45 engraftment was analysed by timely sub-mandibular bleeding procedures. Cells isolated from patient #1 were enriched for CD34 as previously described [24,25]. Cells isolated from patient #2 and #3 were CD3 depleted as previously described [1].

MS5 and MSC co-cultures

CB CD34+ cells were grown in myeloid Gartner's without the ectopic addition of cytokines. CB MLL-AF9 cells were grown under myeloid restricted and lymphoid permissive conditions. More detailed information can be found in the supplementary methods.

Further materials and methods are provided as supplementary information.

Results

Characterization of IL-3 and TPO expressing MSCs *in vitro* and *in vivo*

We recently reported a human niche xenograft model in which MSCs are coated on scaffolds that are subcutaneously implanted in mice to generate humanized bone marrow niches [1,3,23]. Here, we wished to evaluate whether genetically engineered MSCs can be used in this model and provide tools to perform gene-function analyses to study the importance of niche factors for normal and malignant human hematopoiesis.

Transcriptome studies of primary MSCs revealed that a variety of cytokines and growth factors are produced, but some critically important cytokines such IL-3 and TPO are not (Fig. 1A, Supplemental Fig. 1A) [26] and our own unpublished MSC transcriptome studies (data not shown, submitted) confirmed these findings. We transduced primary human MSCs with lentiviral vectors expressing human IL-3 or TPO (Fig. 1B) and tNGFR positive cells were sorted, stored and used for further experiments (Supplemental Fig. 1B). Conditioned supernatant (spnt) of cyto-MSC, mixed with normal MSCs in a range of 1-20%, was used to stimulate the IL-3 and TPO dependent MO-7e cell line for 15 min, after which lysates were analysed for activated STAT5. As controls, cells were stimulated with 1-5 ng/ml IL-3 or TPO as indicated (Fig. 1C). Stimulation with as little as 1% of IL-3 conditioned medium and 5% of TPO conditioned medium induced STAT5 phosphorylation to comparable levels as stimulation with 1 ng/ml of these cytokines, suggesting that the concentration in conditioned media ranged from 10-50 pg/ml. Similarly, MS5 lines were generated that produced IL-3 or TPO (cyto-MS5).

Next, stromal co-cultures were performed to functionally evaluate genetically engineered MSCs and MS5 murine bone marrow stromal cells. Empty vector (EV)-

transduced or non-transduced control stromal cells were mixed with cytokine-producing stromal cells at various ratios. While the presence of IL-3 led to increased proliferation along the myeloid lineage, secretion of TPO resulted in the expansion and maintenance of a more immature phenotype as read out by the percentage and absolute cell counts of $CD34^+$ cells, progenitor activity in CFC assays of cells taken at day 7, 14 and 28 from stromal co-cultures, and morphological analysis by cytospins and MGG staining (Fig. 1D-H, Supplemental Fig. 1C-G). In particular the combination of IL-3- and TPO-producing stroma was most efficient in expanding immature $CD34^+$ progenitor cells (Fig. 1D-H, Supplemental Fig. 1C-G). Importantly, cyto-MSCs were still capable to differentiate and form bone *in vivo* and HE staining indicated that a normal morphology of the scaffolds was obtained including the presence of adipocytes, various stromal components and blood vessels (Fig.1I, Supplemental Fig. 2B). Expression of IL-3 and tNGFR was also confirmed by immunohistochemistry 6 weeks after implantation (Fig. 1J).

Figure 1

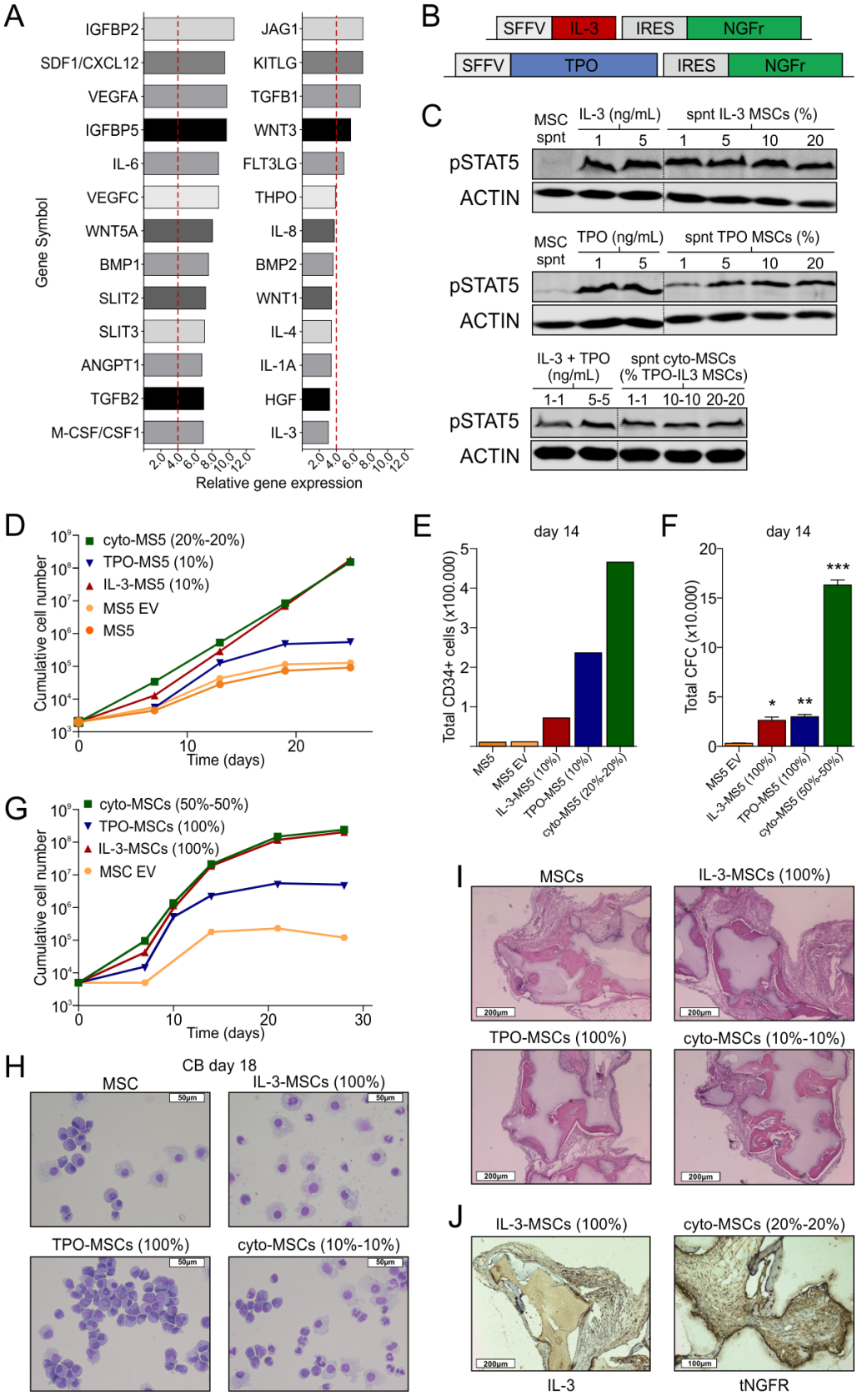
A
IGFBP2
SDF1/CXCL12
VEGFA
IGFBP5
IL-6
VEGFC
WNT5A
BMP1
SLIT2
SLIT3
ANGPT1
TGFB2
M-CSF/CSF1
JAG1
KITLG
TGFB1
WNT3
FLT3LG
THPO
IL-8
BMP2
WNT1
IL-4
IL-1A
HGF
IL-3
Gene Symbol
2.0 4.0 6.0 8.0 10.0 12.0
Relative gene expression
B
SFFV
IL-3
IRES
NGFr
SFFV
TPO
IRES
NGFr
C
MSC spnt
IL-3 (ng/mL)
spnt IL-3 MSCs (%)
1 5 1 5 10 20
pSTAT5
ACTIN
MSC spnt
TPO (ng/mL)
spnt TPO MSCs (%)
1 5 1 5 10 20
pSTAT5
ACTIN
IL-3 + TPO (ng/mL)
spnt cyto-MSCs (% TPO-IL3 MSCs)
1-1 5-5 1-1 10-10 20-20
pSTAT5
ACTIN
D
cyto-MS5 (20%-20%)
TPO-MS5 (10%)
IL-3-MS5 (10%)
MS5 EV
MS5
Cumulative cell number
Time (days)
E
day 14
Total CD34+ cells (x100.000)
MS5
MS5 EV
IL-3-MS5 (10%)
TPO-MS5 (10%)
cyto-MS5 (20%-20%)
F
day 14
Total CFC (x10.000)
*
**
***
MS5 EV
IL-3-MS5 (100%)
TPO-MS5 (100%)
cyto-MS5 (50%-50%)
G
cyto-MSCs (50%-50%)
TPO-MSCs (100%)
IL-3-MSCs (100%)
MSC EV
Cumulative cell number
Time (days)
H
CB day 18
MSC
IL-3-MSCs (100%)
TPO-MSCs (100%)
cyto-MSCs (10%-10%)
50µm
I
MSCs
IL-3-MSCs (100%)
TPO-MSCs (100%)
cyto-MSCs (10%-10%)
200µm
J
IL-3-MSCs (100%)
cyto-MSCs (20%-20%)
200µm
100µm
IL-3
tNGFR

Figure 1, Characterization of IL-3 and TPO expressing MSCs *in vitro* and *in vivo*

A) MSC gene expression profile of selected growth factors and cytokines (GO: secreted). **B)** Schematic representation of the two lenti-viral vectors carrying IL-3 and THPO. **C)** Western blot on M-O7e whole-cell lysate showing the activation of pSTAT5 upon the manual addition of IL-3 and/or TPO, the supernatant of MSCs or a mixture of cyto-MSCs with normal MSCs in different ratios. **D)** Growth curve of $CD34^+$ CB isolated cells co-cultured with cyto-MS5 mixed in different ratios with normal MS5. MS5 EV transduced cells were used as control **E)** $CD34^+$ cumulative count of the CB co-culture with MS5 at day 14. **F)** CFC-analysis, cumulative colony count (technical triplicate, ±s.d.) from the CB co-culture with MS5 at day 14. **G)** Growth curve of $CD34^+$ CB isolated cells co-cultured with cyto-MSCs mixed in different ratios with normal MSCs. **H)** MGG staining of the CB co-culture with MSCs at day 18. **I)** H&E staining of huBM-sc coated with different ratio of normal MSCs, IL-3- or TPO-expressing MSCs or a mixture of cyto-MSCs and normal MSCs after 6 weeks *in vivo*. **J)** IHC staining of IL-3 and tNGFR of cyto-MSCs after 6 weeks *in vivo*. * $p \leq 0.05$, ** $p \leq 0.01$, *** $p \leq 0.001$, paired Student *t* test.

Leukemic cells engraft in human cytokine producing bone marrow scaffolds and recapitulate patient phenotype

Next, engraftment of primary human acute leukemic cells upon direct injection in the scaffolds was evaluated. Scaffolds were coated with 60% normal MSCs, 20% IL-3- and 20% TPO-expressing MCSs (cytoBM-sc), or only with normal MSCs as published previously (huBM-sc) [1]. Three different patient samples were investigated, including

an AML, a B-ALL and a BAL sample (Supplemental Table 1). Leukemic $CD34^+$ cells were injected between 6-8 weeks after subcutaneous implantation of the ectopic engineered BM niches. Efficient engraftment was observed for all leukemia samples in both the huBM-sc or cytoBM-sc models with comparable kinetics (Fig. 2A). The FACS immunophenotype of leukemic cells grown in scaffolds was compared to that of the original patient sample. AML patient #1 presented with a FLT3-ITD and an NPM-MLF1 fusion at diagnosis, with 54% $CD34^+$ cells, 79% $CD33^+$ and 2% $CD19^+$ cells. Leukemia developed in both the huBM-sc or cytoBM-sc models with palpable tumors originating from the scaffolds and infiltration of human $CD45^+$ cells in the mouse compartments such BM, spleen and liver was observed as well. For this sample, the immunophenotype of the original patient sample was well preserved in both the normal and cytokine humanized niches (Fig. 2B). B-ALL patient #2 contained an MLL-AF4 translocation with 99% $CD19^+$ cells at diagnosis. For this sample, CD34-positivity of engrafting cells was better preserved in the cytoBM-sc model compared to the huBM-sc (Fig. 2A) and murine niche environment (data not shown). Lastly, we analysed patient #3 who presented a BAL with complex karyotype (Supplemental Table 1). Overall, cells retrieved from the cytoBM-sc displayed an immunophenotype that or more closely resembled the phenotype of the patient at diagnosis, in particular with regard to expression levels of $CD33^+$ and $CD38^+$ (Fig. 2A, 2C).

Figure 2

A

	de novo	huBM-sc	cytoBM-sc	*de novo*	huBM-sc	cytoBM-sc	*de novo*	huBM-sc	cytoBM-sc
Patient ID	#1	#1	#1	#2	#2	#2	#3	#3	#3
Time of sacrifice (wks)		19.0 ± 1.0 (n=3)	22.0 (n=1)		21.5 ± 4.9 (n=2)	26.3 ± 8.1 (n=2)		28 (n=1)	23.0 ± 2.6 (n=3)
CD34	54	61	64	15	<1	9	74	97	97
CD38	85	73	93	99	100	100	98	17	68
CD33	100	100	100	2	<1	3	98	37	98
CD19	6	9	7	99	100	100	84	99	98
CD11b	27	6	4	<1	1	<1	9	<1	1
CD14	3	0	7	2	12	12	12	<1	20
CD11c	32	9	11	<1	<1	1	<1	1	0
CD13	86	77	81	3	5	4	3	3	25
CD15	11	11	4	39	53	29	10	13	5
CD117	83	89	97	<1	1	1	<1	<1	1

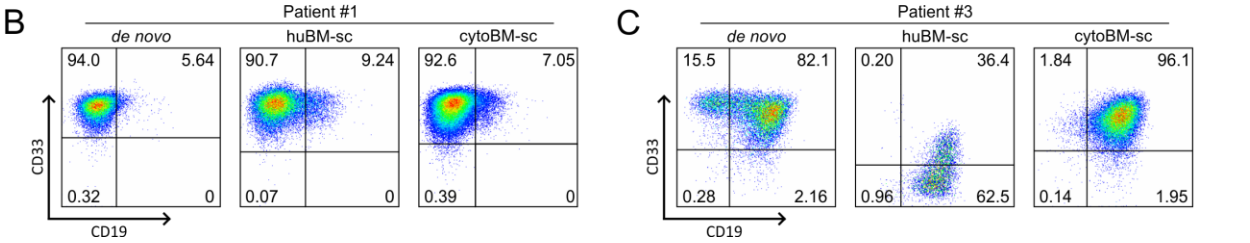

Figure 2, Leukemic cells engraft in cytoBM-sc and recapitulate patients phenotype A) Immunophenotype of 3 patients; *de novo* (after thawing), cells retrieved from human niches of huBM-sc NSG and cytoBM-sc NSG models. **B-C)** FACS analyses comparing immunophenotype of patient #1 **(B)** and patient #3 **(C)** *de novo,* in huBM-sc and cytoBM-sc.

CB MLL–AF9 cells can transform along myeloid and lymphoid lineages on cyto-MSC co-cultures.

CB $CD34^+$ cells transduced with MLL-AF9 can be transformed along the myeloid or lymphoid lineage depending on extrinsic cues [15,27]. We have previously shown that while in the normal NSG xenograft model MLL-AF9-induced transformation *in vivo* is heavily lymphoid biased, more myeloid transformation is observed in the humanized niche scaffold model [3,27]. Nevertheless, since in particular IL-3 was shown to be important for MLL-AF9 induced human AML in xenografts, and not produced by our

MSCs (Fig. 1A), we investigated the leukemic transformation potential of MLL-AF9 transduced CB $CD34^+$ cells in our cytoBM-sc model.

To study this, we first cultured MLL-AF9-transduced CB cells *in vitro* on MSCs or a mixture of cyto-MSCs and MSCs supplemented with cytokines under myeloid-restricted or lymphoid permissive conditions. Rapid transformation was observed under all growth conditions (Fig. 3A). We did not observe any differences in growth between the myeloid-restricted culture conditions and all cells remained $CD33^+$ under both conditions (Fig. 3A-B). Under lymphoid-permissive conditions CB MLL-AF9 cells expanded faster on MSCs with lymphoid cytokines compared to the cyto-MSCs (Fig. 3A). CB MLL-AF9 cells underwent full lymphoid transformation on MSCs with the addition of lymphoid cytokines, whereas in the cyto-MSCs grown under lymphoid-permissive conditions both lymphoid and myeloid clones were expanding (Fig. 3C). A typical feature of MLL-AF9 transformed cells is the formation of large cobblestone areas as was observed in both the normal MSC as well as the cyto-MSC co-cultures (Fig. 3D). These data indicate that both MLL-AF9-induced myeloid as well as lymphoid transformation can be achieved *in vitro* on cyto-MSCs, whereby transformation appears to be more balanced towards the myeloid lineage compared to co-cultures on normal MSCs.

Figure 3

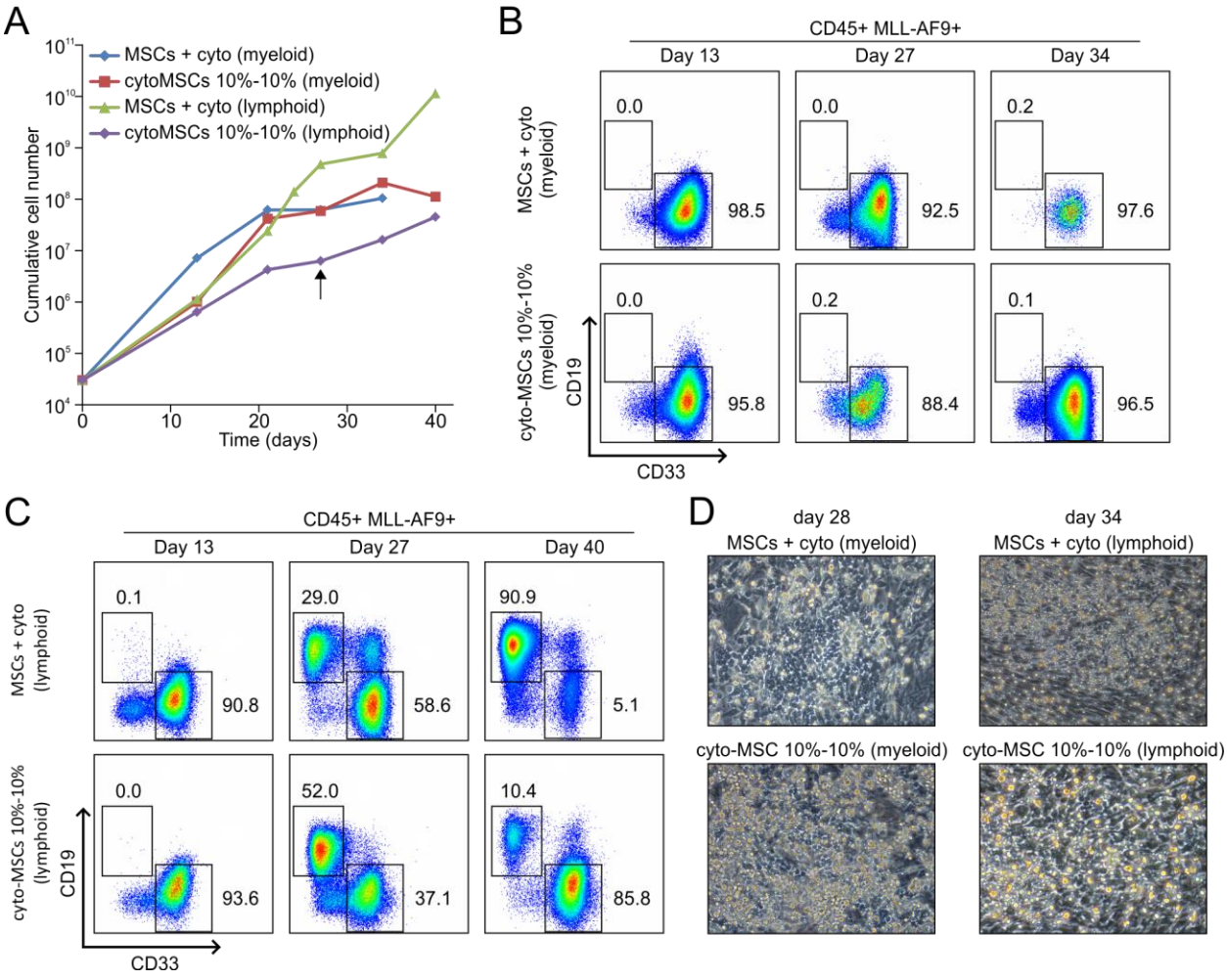

Figure 3, Cyto-MSC co-cultures with CB MLL–AF9 cells allow immortalization along the myeloid and lymphoid lineage

A) Total cumulative expansion of CB MLL-AF9 cells is shown. Arrow indicates when the cells were replated on fresh stroma. **B-C)** CD33 and CD19 expression in suspension cells for the myeloid co-cultures **(B)** and lymphoid co-cultures **(C)** at multiple time points. **D)** Cobblestone area-forming cells underneath MSC stroma of myeloid and lymphoid co-cultures.

Increased frequency of MLL-AF9-induced myeloid leukemia in cytoBM-sc implanted mice

We evaluated the *in vivo* MLL-AF9-driven leukemogenesis upon direct injection into cytoBM-sc NSG mice and compared that to our previously published models (intravenously (IV) injected NSG mice and scaffold injected (ISC) huBM-sc) (Fig. 4A). In cytoBM-sc mice (n=11), 3 out of 4 implanted scaffolds were injected with $3x10^5$ unsorted CB transduced MLL-AF9 cells, comparable to cell numbers that were injected into previously published IV or huBM-sc models. The transduction efficiency at the day of injection was approximately 15% (data not shown). All mice developed a fatal leukemia in 20-52 weeks, with a significantly longer latency compared to the previously used models (IV NSG vs cytoBM-sc: p=0.017, huBM-sc vs cytoBM-sc: p=0.046). Unexpectedly, out of the 33 injected scaffolds only 8 scaffolds developed palpable tumors (24%), while in the huBM-sc model this percentage was 79% (Fig. 4B). Nevertheless, in all the injected cytoBM-sc that did not develop tumors, we could confirm the presence of human cells by IHC staining for $CD45^+$ (Supplemental Fig. 2A), of which a representative example is shown for mouse #5 cytoBM-sc1 (Fig. 4C), confirming that human cells were injected initially. The scaffold that did develop a tumor in mouse #5 (cytoBM-sc3) was analysed by IHC staining confirming positivity for CD45, CD33 and IL-3 (Fig. 4C). Overall, the frequency of AML, B-ALL and mixed AML/B-ALL cells within the scaffolds was comparable between huBM-sc and cytoBM-sc models (Fig. 4D).

We hypothesize that the lower rate of tumors formed on the scaffolds of cytoBM-sc mice might possibly be attributed to potentially high levels of exogenous IL-3 and TPO that

would induce differentiation or loss of long-term self-renewal properties. As confirmed by IHC staining for the mouse endothelial marker CD31 and VwF, cytoBM-sc were well vascularized, allowing leukemic clones to migrate from the site of injection to mouse compartments (PB, BM, spleen, liver) (Supplemental Fig. 2B). In fact, all mice developed an enlarged spleen, with an average weight of 0.82 ± 0.31 g (Supplemental Fig. 2C). In contrast to our previous IV and huBM-sc models, differences in the leukemic phenotypes were observed in the mouse compartments. $CD33^{+}/CD19^{-}$ AML cells were detected in the PB, BM, spleen and liver of mouse #10 (Fig. 4D-E and Supplemental Fig. 2A). Even though this was only one example, such exclusively myeloid cells in PB, spleen, liver or BM had never been observed in any of our previous models (Fig. 4D, [3,27]). Furthermore, 20% of the mice displayed mixed B-ALL/AML clones in the spleen or liver, again a feature that was never observed in previous studies (Fig. 4D-E [3,27]). In the murine BM niche, the mixed B-ALL/AML frequency was in line with what was observed in the previous models (Fig. 4D-E). MGG staining was performed on tissues to confirm the myeloid and/or lymphoid cells and a representative example of mouse #1 with mixed B-ALL/AML is shown (Fig. 4F).

Although MSCs are not known to migrate efficiently from one organ to another, we questioned whether some MSCs might have migrated to the liver in the mouse that displayed exclusively AML cells (mouse #10). While we could detect the presence of CD45-expressing cells and IL-3, indicating engraftment of human cells as well as the presence of human IL-3, no tNGFR positive cells were detected (Fig. 4G), providing no evidence for the migration of MSCs to the liver. Instead, tNGFR positive cells were detected in the scaffolds (Fig. 1J). Overall, these data indicate that CB MLL-AF9 cells

can engraft in the cytoBM-sc model albeit with longer latency and lower frequency, while in the organs of these mice the balance in lineage output is shifted somewhat towards more myeloid or mixed AML/B-ALL phenotypes.

Figure 4

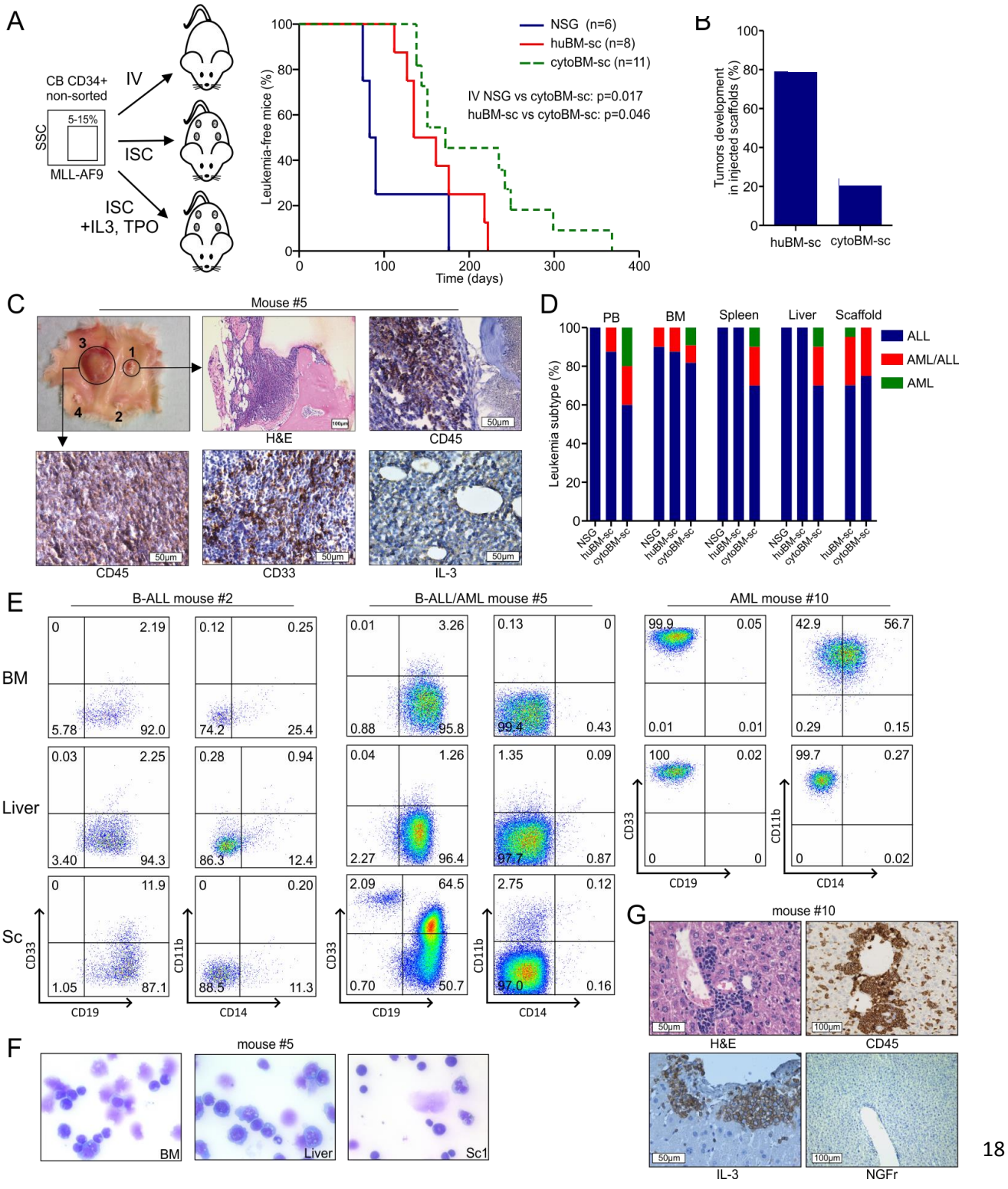

Figure 4, Increased frequency of MLL-AF9-induced myeloid leukemia in cytoBM-sc implanted mice

A) Schematic representation of the different models injected with CB MLL-AF9 cells: IV injected NSG mice, ISC injected huBM-sc and ISC injected cytoBM-sc. Kaplan–Meier survival curves of CB MLL-AF9-injected mice, displaying the differences in kinetics of leukemia development. **B)** Percentage of tumor formation in injected scaffolds in huBM-sc and cytoBM-sc. **C)** Picture depicting tumor initiated on scaffold 3 from mouse #5, with IHC for CD45, CD33 and IL-3 staining for scaffold 3 and HE and CD45 IHC staining of scaffold 1, that did not develop a solid tumor but displayed human cell engraftment. **D)** Frequencies of leukemic phenotypes observed in three different experimental set ups: IV injected NSG mice, ISC injected huBM-sc and ISC injected cytoBM-sc. **E)** FACS analyses of CD45+MLL-AF9+ cells from BM, liver and scaffold of ISC injected cytoBM-sc mice displaying different leukemic phenotypes. **F)** MGG staining of B-ALL/AML MLL-AF9 cells from BM, liver, and huBM-sc (mouse#5), 40x magnification. **G)** IHC for CD45, CD33, IL-3 and tNGFR on liver sections from mouse #10.

Lymphoid clones outcompete myeloid clones in secondary transplantation

In our previously published studies using the IV NSG and huBM-sc models, CB MLL-AF9 B-ALL cells could readily engraft in secondary recipients [3,27], while secondary engraftment of myeloid $CD33^+$ clones was not achieved. For example, in an IV model in which we observed a mixed AML and B-ALL phenotype, we sorted $CD33^+/CD19^-$ and $CD19^+/CD33^-$ populations and transplanted them IV into secondary mice without scaffolds. While the $CD19^+/CD33^-$ clones readily induced secondary B-ALL within 8

weeks after transplantation, the $CD33^+/CD19^-$ clones engrafted with much slower kinetics (Supplemental Fig. 3A). At early phases $CD33^+/CD19^-$ myeloid cells were still observed in the PB of these mice, however, lymphoid $CD19^+/CD33^-$ clones appeared as well, became more dominant over time, and at the time of sacrifice at week 16 the mice succumbed of B-ALL and not AML (Supplemental Fig. 3A). LM-PCRs indicated that a minor fraction of lymphoid $CD19^+/CD33^-$ B-ALL cells contaminated the myeloid $CD33^+/CD19^-$ sorted population and it was exactly this population that generated the B-ALL (Supplemental Fig. 3B). These data clearly highlight the lymphoid bias of routinely used NSG xenograft mouse models.

We evaluated the self-renewal potential of CB MLL-AF9 AML cells generated in cytoBM-sc mice. We sorted $GFP^+/CD45^+/CD33^+$ cells from BM, spleen, liver and scaffold 1 of mouse #1 and scaffold 3 of mouse #5 (Fig. 5A, Supplemental Fig. 2A). $1.1x10^5$ cells from BM, spleen and liver were injected per scaffold, and in total 2 scaffolds were injected, while $0.9x10^5$ cells from scaffold of mouse #1 and #5 were injected in a single scaffold of secondary cytoBM-sc mice. Secondary leukemic engraftment was observed only in the mouse injected with AML cells derived from BM. Tumor formation was observed in one of the two injected scaffolds and infiltration of CB MLL-AF9-positive cells was also observed in the BM, spleen and liver. Despite the fact that the injected cells were sorted for the myeloid marker $CD33^+$, the secondary mouse developed $CD19^+$ B-ALL. As previously observed, this may be explained by a small contamination of $CD19^+$ cells during the sorting procedure (data not shown). One secondary mouse transplanted with AML cells derived from spleen died during the course of the experiment and the remaining 3 mice were sacrificed 45 weeks after

injection without signs of disease. These results indicate that despite the presence of an engineered human niche microenvironment providing IL-3 and TPO, MLL-AF9-induced transformation of neonatal CB CD34^{+} cells remains biased towards CD19^{+} B-ALL.

Figure 5

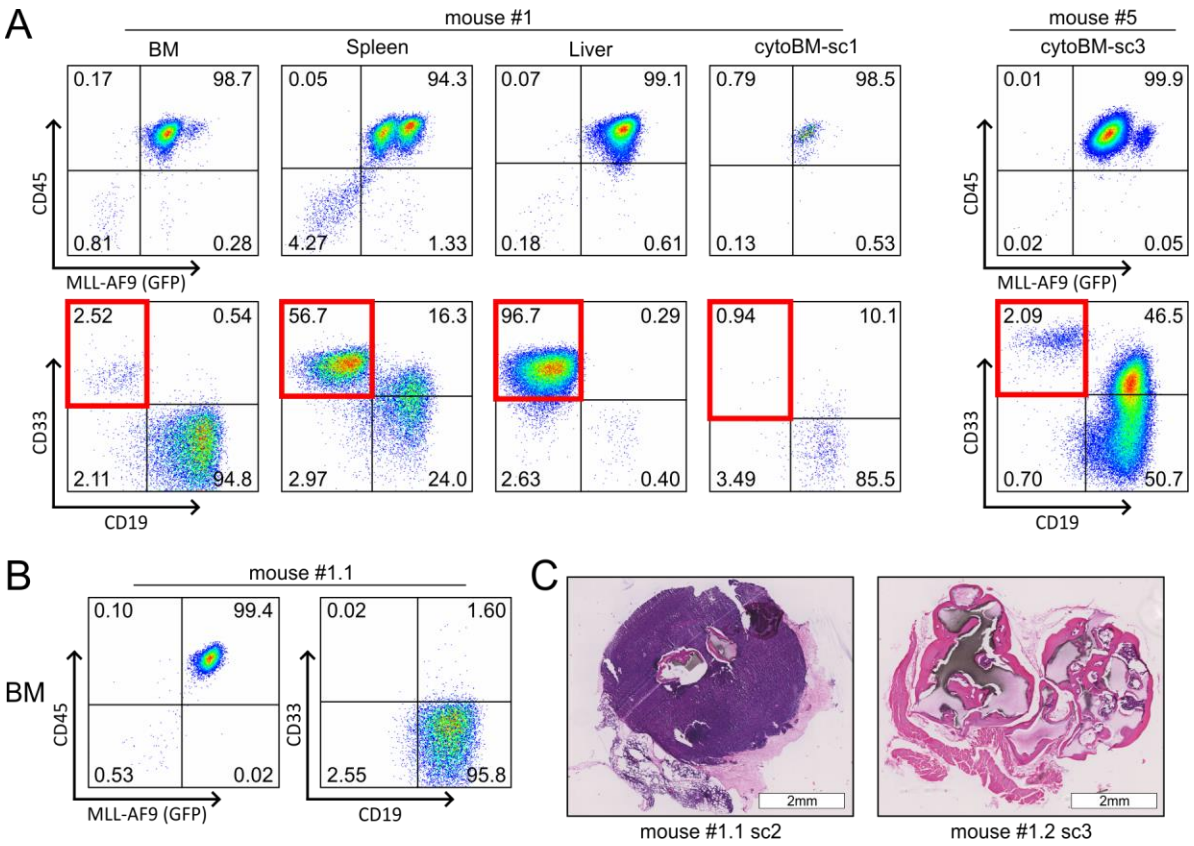

Figure 5 Lymphoid clones outcompete myeloid clones in secondary transplantation

A) FACS analyses of CB MLL-AF9 cells from BM, liver, spleen and huBM-sc of ISC injected cytoBM-sc (mouse #1) and huBM-sc (mouse #5). Red boxes indicate the sorted cells injected in secondary recipients. **B)** FACS analyses of MLL-AF9 cells from BM ISC injected secondary cytoBM-sc (mouse #1.1).**C)** H&E staining of engrafted secondary cytoBM-sc (mouse #1.1) and non-engrafted cytoBM-sc (mouse #1.2).

Discussion

In order to improve the *in vivo* xenograft modelling of human hematological malignancies, several laboratories have begun to build humanized microenvironments in xenograft mice by making use of human mesenchymal stromal cells in order to provide better niches in which leukemic cells can engraft [1-3,23,28-31]. In this study, we aimed to further develop our previously described huBM-sc model [1,3,23]using human MSCs that we genetically engineered to express cytokines that were not expressed in these cells. We engineered MSCs stably expressing human IL-3 or human TPO, and tested these functionally. *In vitro,* these IL-3 and TPO-producing MSCs were superior in expanding human cord blood (CB) $CD34^+$ hematopoietic stem/progenitor cells. Furthermore, MLL-AF9-transduced CB $CD34^+$ cells could efficiently be transformed along myeloid or lymphoid lineages on IL-3 and TPO-producing MSCs. These data indicate that these genetically engineered MSCs are sufficient to allow either myeloid or lymphoid transformation without the need for additional exogenous cytokines. Importantly, in the absence of exogenous cytokines, non-engineered MSCs or MS5 are not sufficient to allow *in vitro* transformation of MLL-AF9-transduced CB cells ([27] and data not shown). We did notice that under lymphoid-permissive conditions the balance of MLL-AF9-induced transformation appeared to be shifted towards the myeloid lineage at later timepoints in comparison to when exogenous cytokines were added (Fig. 3C).

Next, we assessed the ability of cyto-MSCs to differentiate *in vivo*. Six weeks after implantation, mice were sacrificed and scaffolds were analysed. No differences in the

ability of forming bone, fat tissue and stromal component were observed compared to normal MSCs.

We then studied the engraftment of three primary AML, B-ALL and BAL patient samples in our new IL3/TPO-producing cytoBM-sc model to our previous huBM-sc models. All three tested samples efficiently engrafted in the cytoBM-sc model, with latencies and immunophenotypes that did not significantly differ from what we previously had observed in our huBM-sc model (Fig.2 and [1]). The main differences were that immature $CD34^+$ cells for the B-ALL sample were better preserved in our new cytoBM-sc model, and the same was true for the myeloid $CD33^+$ immune phenotype for the BAL patient sample. Furthermore, engraftment of MLL-AF9-transduced CB cells was evaluated in the new cytoBM-sc model since it had been shown that the lineage fate of MLL-AF9 expressing cells can be dictated by environmental cues [15,27], and we compared these data to our previous huBM-sc models and IV models [27]. Injection of MLL-AF9-transduced CB cells into the scaffolds of cytoBM-sc models resulted in the development of a fatal leukemia in all the experimental animals. At sacrifice, mice displayed both the myelomonocytic and B-ALL immunophenotypes that are also observed in MLL-AF9 pediatric patients. Surprisingly, the efficiency of tumor formation on the injected scaffolds themselves was reduced by ~55% in the cytoBM-sc model compared to the previous huBM-sc model. A possible explanation for this might be that the local concentrations of IL-3 and TPO produced by the genetically engineered MSCs would be non-physiological, resulting either in the differentiation or the loss of self-renewal properties, or potentially in the migration of leukemic cells to other mouse niches where the cytokine concentrations would be less high. In fact, for the first time

we detected complete myeloid AML clones in PB, BM, spleen and liver. Also mixed B-ALL/AML clones were observed for the first time in spleen and liver. Although we have not been able to quantify the exact levels of exogenous cytokines in the different murine tissues, we have been able to detect human IL-3 in the liver of mice transplanted with cytoBM-sc by IHC. This suggests that increased levels of IL-3 might indeed underlie the higher frequency of myeloid and mixed clones observed in murine tissues, but further studies are needed to clarify these issues. As already observed in the IV NSG model and in the ISC huBM-sc model, also in the cytoBM-sc model $CD33^{+}$-sorted myeloid clones failed to self-renew in secondary recipients, while B-ALL clones could readily engraft and give rise to secondary leukemia. This finding was somewhat unexpected and suggests that the presence of a modified human microenvironment that overexpresses IL-3 and TPO does not allow myeloid clones to self-renew properly, but a further fine-tuning of the levels of cytokines produced in the humanized niche might be required to solve these issues. The present study does clearly indicate that the humanized scaffold xenograft model allows for relatively simple genetic engineering of the bone marrow microenvironment. As such, this approach will be very useful to functionally study the importance of niche factors for normal and malignant human hematopoiesis.

Acknowledgements

The authors thank Prof. dr. J. J. Erich and Dr. A. van Loon and colleagues (Departments of Obstetrics, University Medical Center Groningen and Martini Hospital Groningen) for collecting cord blood. This work was supported by grants from the EU

(FP7-PEOPLE-2010-ITN EuroCancer StemCell Training network) and European Research Council (ERC-2011-StG 281474-huLSCtargeting).

Reference List

1. Antonelli A, Noort WA, Jaques J, et al. Establishing human leukemia xenograft mouse models by implanting human bone marrow-like scaffold-based niches. Blood. 2016;128(25):2949-59.

2. Reinisch A, Thomas D, Corces MR, et al. A humanized bone marrow ossicle xenotransplantation model enables improved engraftment of healthy and leukemic human hematopoietic cells. Nat Med. 2016.

3. Sontakke P, Carretta M, Jaques J, et al. Modeling BCR-ABL and MLL-AF9 leukemia in a human bone marrow-like scaffold-based xenograft model. Leukemia. 2016;doi: 10.1038/leu.2016.108. [Epub ahead of print].

4. Ito M, Hiramatsu H, Kobayashi K, et al. NOD/SCID/gamma(c)(null) mouse: an excellent recipient mouse model for engraftment of human cells. Blood. 2002;100(9):3175-82.

5. Ishikawa F, Yasukawa M, Lyons B, et al. Development of functional human blood and immune systems in NOD/SCID/IL2 receptor {gamma} chain(null) mice. Blood. 2005;106(5):1565-73.

6. Barabe F, Kennedy JA, Hope KJ, Dick JE. Modeling the initiation and progression of human acute leukemia in mice. Science. 2007;316(5824):600-4.

7. Townsend EC, Murakami MA, Christodoulou A, et al. The Public Repository of Xenografts Enables Discovery and Randomized Phase II-like Trials in Mice. Cancer Cell. 2016;30(1):183.

8. Vargaftig J, Taussig DC, Griessinger E, et al. Frequency of leukemic initiating cells does not depend on the xenotransplantation model used. Leukemia. 2012;26(4):858-60.

9. Sanchez PV, Perry RL, Sarry JE, et al. A robust xenotransplantation model for acute myeloid leukemia. Leukemia. 2009;23(11):2109-17.

10. Wang K, Sanchez-Martin M, Wang X, et al. Patient-derived xenotransplants can recapitulate the genetic driver landscape of acute leukemias. Leukemia. 2017;31(1):151-8.

11. Nicolini FE, Cashman JD, Hogge DE, Humphries RK, Eaves CJ. NOD/SCID mice engineered to express human IL-3, GM-CSF and Steel factor constitutively mobilize engrafted human progenitors and compromise human stem cell regeneration. Leukemia. 2004;18(2):341-7.

12. Ito R, Takahashi T, Katano I, et al. Establishment of a human allergy model using human IL-3/GM-CSF-transgenic NOG mice. J Immunol. 2013;191(6):2890-9.

13. Brehm MA, Racki WJ, Leif J, et al. Engraftment of human HSCs in nonirradiated newborn NOD-scid IL2rgamma null mice is enhanced by transgenic expression of membrane-bound human SCF. Blood. 2012;119(12):2778-88.

14. Wunderlich M, Chou FS, Link KA, et al. AML xenograft efficiency is significantly improved in NOD/SCID-IL2RG mice constitutively expressing human SCF, GM-CSF and IL-3. Leukemia. 2010;24(10):1785-8.

15. Wei J, Wunderlich M, Fox C, et al. Microenvironment determines lineage fate in a human model of MLL-AF9 leukemia. Cancer Cell. 2008;13(6):483-95.

16. Rongvaux A, Willinger T, Martinek J, et al. Development and function of human innate immune cells in a humanized mouse model. Nat Biotechnol. 2014;32(4):364-72.

17. Rongvaux A, Willinger T, Takizawa H, et al. Human thrombopoietin knockin mice efficiently support human hematopoiesis in vivo. Proc Natl Acad Sci U S A. 2011;108(6):2378-83.

18. Strowig T, Rongvaux A, Rathinam C, et al. Transgenic expression of human signal regulatory protein alpha in Rag2-/-gamma(c)-/- mice improves engraftment of human hematopoietic cells in humanized mice. Proc Natl Acad Sci U S A. 2011;108(32):13218-23.

19. Willinger T, Rongvaux A, Takizawa H, et al. Human IL-3/GM-CSF knock-in mice support human alveolar macrophage development and human immune responses in the lung. Proc Natl Acad Sci U S A. 2011;108(6):2390-5.

20. Willinger T, Rongvaux A, Strowig T, Manz MG, Flavell RA. Improving human hemato-lymphoid-system mice by cytokine knock-in gene replacement. Trends Immunol. 2011;32(7):321-7.

21. Goyama S, Wunderlich M, Mulloy JC. Xenograft models for normal and malignant stem cells. Blood. 2015.

22. Theocharides AP, Rongvaux A, Fritsch K, Flavell RA, Manz MG. Humanized hemato-lymphoid system mice. Haematologica. 2016;101(1):5-19.

23. Groen RW, Noort WA, Raymakers RA, et al. Reconstructing the human hematopoietic niche in immunodeficient mice: opportunities for studying primary multiple myeloma. Blood. 2012;120(3):e9-e16.

24. Rizo A, Olthof S, Han L, et al. Repression of BMI1 in normal and leukemic human CD34(+) cells impairs self-renewal and induces apoptosis. Blood. 2009;114(8):1498-505.

25. Schuringa JJ, Chung KY, Morrone G, Moore MA. Constitutive activation of STAT5A promotes human hematopoietic stem cell self-renewal and erythroid differentiation. J Exp Med. 2004;200(5):623-35.

26. Markov V, Kusumi K, Tadesse MG, et al. Identification of cord blood-derived mesenchymal stem/stromal cell populations with distinct growth kinetics, differentiation potentials, and gene expression profiles. Stem Cells Dev. 2007;16(1):53-73.

27. Horton SJ, Jaques J, Woolthuis C, et al. MLL-AF9-mediated immortalization of human hematopoietic cells along different lineages changes during ontogeny. Leukemia. 2013;27(5):1116-26.

28. Chen Y, Jacamo R, Shi YX, et al. Human extramedullary bone marrow in mice: a novel in vivo model of genetically controlled hematopoietic microenvironment. Blood. 2012;119(21):4971-80.

29. Francis OL, Milford TA, Beldiman C, Payne KJ. Fine-tuning patient-derived xenograft models for precision medicine approaches in leukemia. J Investig Med. 2016;64(3):740-4.

30. Milford TA, Su RJ, Francis OL, et al. TSLP or IL-7 provide an IL-7Ralpha signal that is critical for human B lymphopoiesis. Eur J Immunol. 2016;46(9):2155-61.

31. Francis OL, Milford TA, Martinez SR, et al. A novel xenograft model to study the role of TSLP-induced CRLF2 signals in normal and malignant human B lymphopoiesis. Haematologica. 2016;101(4):417-26.